Experimental Brain Research (2019) 237:3375–3390
https://doi.org/10.1007/s00221-019-05683-z

RESEARCH ARTICLE

The role of cortical areas hMT/V5+ and TPJ on the magnitude of representational momentum and representational gravity: a transcranial magnetic stimulation study

Nuno Alexandre De Sá Teixeira[1,2,3] · Gianfranco Bosco[1,2] · Sergio Delle Monache[1,2] · Francesco Lacquaniti[1,2]

Received: 12 February 2019 / Accepted: 7 November 2019 / Published online: 14 November 2019

Abstract

The perceived vanishing location of a moving target is systematically displaced forward, in the direction of motion—representational momentum—, and downward, in the direction of gravity—representational gravity. Despite a wealth of research on the factors that modulate these phenomena, little is known regarding their neurophysiological substrates. The present experiment aims to explore which role is played by cortical areas hMT/V5+, linked to the processing of visual motion, and TPJ, thought to support the functioning of an internal model of gravity, in modulating both effects. Participants were required to perform a standard spatial localization task while the activity of the right hMT/V5+ or TPJ sites was selectively disrupted with an offline continuous theta-burst stimulation (cTBS) protocol, interspersed with control blocks with no stimulation. Eye movements were recorded during all spatial localizations. Results revealed an increase in representational gravity contingent on the disruption of the activity of hMT/V5+ and, conversely, some evidence suggested a bigger representational momentum when TPJ was stimulated. Furthermore, stimulation of hMT/V5+ led to a decreased ocular overshoot and to a time-dependent downward drift of gaze location. These outcomes suggest that a reciprocal balance between perceived kinematics and anticipated dynamics might modulate these spatial localization responses, compatible with a push–pull mechanism.

Keywords Representational momentum · Representational gravity · Medio-temporal area · Temporo-parietal junction · Theta-burst stimulation

Introduction

An influential idea in recent research on the perception of moving objects is that dynamic regularities of physical systems have representational counterparts. These are thought to be instantiated in dedicated neural structures and account for a set of assumptions and expectations which guide and fine-tune the perceived features. Hypothetically, and by virtue of the highly regular characteristics of physical dynamics, observers could capitalize on that predictability, by internally modelling its effects and, consequently, anticipating future states of events. Notwithstanding, the functioning of such representational analogues could also result in systematic errors.

If an observer is asked to indicate the perceived vanishing location of a moving object, the response is usually found to be displaced forward, in the direction of motion, and downward, in the direction of gravity. These errors have been linked to the functioning of representational analogues of momentum and gravity and coined, accordingly, as representational momentum (RM; Freyd and Finke 1984) and Representational Gravity (RG; Hubbard 1990). Even though several factors are known to modulate the magnitudes of both RM and RG (Hubbard, 2005, 2010, 2014, 2015), little is known regarding their neurophysiological substrates.

Communicated by Melvyn A. Goodale.

✉ Nuno Alexandre De Sá Teixeira
de.sa.teixeira@gmail.com

[1] Department of Systems Medicine and Centre of Space Biomedicine, University of Rome 'Tor Vergata', 00133 Rome, Italy

[2] Laboratory of Neuromotor Physiology, IRCCS Santa Lucia Foundation, 00179 Rome, Italy

[3] Department of Education and Psychology, William James Research Center, University of Aveiro, Campus Universitário de Santiago, 3810-193 Aveiro, Portugal

Phenomena of spatial localization

Originally reported in 1984 by Freyd and Finke (1984), RM refers to a perceptual displacement of the last seen position of an object undergoing either implicit, implied, or actual movement. The phenomenon has subsequently been reported for perceptual domains other than the visual (Freyd et al. 1990; Getzmann et al. 2004; Kelly and Freyd 1987), to be modulated by seen kinematics (Freyd and Finke 1985; Freyd and Johnson 1987), type of stimuli events (Freyd 1983; Freyd and Miller 1992; Freyd and Pantzer 1995; Reed and Vinson 1996; Vinson and Reed 2002) and with varying psychophysical tasks (Hubbard and Bharucha 1988).

If, on the one hand, the proliferation of studies on RM reflected on the scope of the literature, on the other hand, it also became evident that the phenomenon is differently affected by several variables, depending on the nature of the task and the type of motion. These findings cast doubts on whether a forward perceptual displacement can, by itself, be unambiguously interpreted as evidencing an analogue of a physical invariant.

As a case in point, RM is systematically reported with implied motion stimuli both when participants have to judge the relative location of a visual probe (henceforth referred to as a "perceptual judgement"; Freyd and Finke, 1984; Freyd and Johnson 1987; but see Kerzel 2002) and when required to displace a visual cursor with the aid of a computer mouse to the perceived vanishing location (henceforth referred to as a "behavioural localization response"; Kerzel 2003a, b). However, with smooth continuous motions, RM emerges with behavioural localization responses (Hubbard and Bharucha 1988), but not consistently when a perceptual judgement is required (see, e.g., De Sá Teixeira et al. 2017, for a null result, and Hubbard 1990, for a significant RM).

Furthermore, it is known that when a smoothly tracked target suddenly vanishes, the eyes keep moving in the same direction and speed for some time, before decelerating and coming to a stop at a position which overshoots the actual offset of the target (Luebke and Robinson 1988; Mitrani and Dimitrov 1978; Pola and Wyatt 1997). This observation led some authors to suggest a causal role of eye movements on RM. Accordingly, given a continuous movement of the target, preventing smooth pursuit eye movements reduces (Kerzel 2003a, c; Müsseler et al. 2002) or supresses (De Sá Teixeira 2016; De Sá Teixeira et al. 2013; Kerzel 2000; Kerzel et al. 2001) RM, a finding which was taken as evidence that, under these conditions, the forward displacement might be strongly linked with the ocular overshoot of the target offset location (Kerzel 2006). Interestingly, if participants must directly point to the vanishing location of the target, constraining eye movements seems to have little effect, and RM is still observed (Ashida 2004; Kerzel and Gegenfurtner 2003), an outcome which has been interpreted as evidence for an action-specific extrapolation of the target kinematics.

The perceived offset of a moving target has also been found to be displaced downward, in the direction of gravity (RG), an effect that has shown considerably more robustness across varying methodologies and types of motion. Some of the first studies on RM, requiring a perceptual judgement regarding the position of a visual probe, reported that static displays depicting unsupported objects (Freyd et al. 1988) or a ball in an incline (Bertamini 1993) lead to significant downward displacements. Likewise, downward implied motions were found to result in a bigger displacement (in comparison with upward implied motions; Nagai et al. 2002). Finally, when people are instructed to locate with a computer mouse the perceived vanishing position of a smoothly moving descending target, forward displacement is bigger in comparison with an ascending target (Hubbard and Bharucha 1988). For horizontally moving objects, people systematically indicate the perceived offset position of the target as lower than it actually was (Hubbard 1990), a bias that emerges even for static stimuli (De Sá Teixeira and Hecht 2014; Hubbard and Ruppel 2002). Finally, and unlike what is the case for RM, constraining eye movements (De Sá Teixeira 2016) or emitting a perceptual judgement instead of a behavioral spatial localization (De Sá Teixeira et al. 2017) does not seem to significantly impact on RG.

Taken together, these outcomes strongly suggest a dissociation of the processes responsible for RM, mostly dependent upon perceived kinematics and ocular and motor mechanics, and RG, conveying mainly putative expected dynamics of the environment (see also Motes et al. 2008), suggesting that disparate neural substrates might be found to modulate these phenomena. However, and although some studies did focus on the neural correlates of RM, no attention to date has been devoted to RG, albeit some parallel research lines do provide some hints as to how gravitational-relevant information is processed in the brain.

Neurophysiology of RM and RG

White et al. (1993) first reported a higher RM for stimuli processed by the right cerebral hemisphere. These researchers employed an inducing sequence of three squares varying in size, implying either a shrinking or expanding motion, presented at fixation. Afterwards, a probe, either consistent or inconsistent with the direction of implied motion, was presented in the left or right visual hemifield and participants required to provide a same/different judgement concerning its size in comparison with the last square of the inducing sequence. Magnitude of RM was found to be significantly

higher when the probe was presented 500 ms after the termination of the inducing sequence and in the left visual field. For longer retention intervals, the magnitude of RM measured for the right hemisphere fell to the value found for the left hemisphere (which produced constant biases). Further support for the involvement of the right cerebral hemisphere has been provided by contrasting the performance of patients with left spatial neglect and right hemisphere damage with no neglect with normal controls in a spatial localization task directed to the offset position of a smoothly moving target (McGeorge et al. 2006). Although all participants showed a forward displacement, for patients with right hemisphere damage the magnitude of RM decreased as a function of distance travelled by the target, being virtually null for the longer lengths.

Static stimuli implying motion (e.g., an image of a hand dropping a mug) have been found not only to lead to RM effects (Freyd 1983; Freyd et al. 1988) but also to significantly increase metabolic activity in the middle-temporal (hMT/V5+) and medial superior temporal (MST) areas—as assessed with fMRI (Kourtzi and Kanwisher 2000; Senior et al. 1999). The involvement of area hMT/V5+ in RM was further tested by applying repetitive transcranial magnetic stimulation between the presentation of a static image implying motion and the presentation of a probe, for which participants had to provide a same/different perceptual judgement (Senior et al. 2002). RM was found to be suppressed with stimulation of hMT/V5+, which was interpreted as evidence for a functional necessity of that cortical area. Notwithstanding, this conclusion is far from clear, for Rao et al. (2004) reported no increased activity in hMT/V5+ using fMRI methodology when observers were instructed to provide a perceptual judgement regarding the last orientation of a rectangle undergoing apparent rotation (in contrast with scrambled sequences implying no regular motion). The discrepancy between the studies by Rao et al. (2004) and those by Senior et al. (1999) and Kourtzi and Kanwisher (2000) seems to be due to the type of stimuli events and the strength of the motion signal: while in the former studies the task consisted in an inducing sequence of rectangles implying a rotational motion, the latter studies used static images with implicit dynamics as stimuli. It remains to be explained why only the implicit motion stimuli would depend on the functioning of hMT/V5+. Among the cortical areas known to be responsive to visual motion (Sunaert et al. 1999), hMT/V5+ is by far the one which has received more attention, being systematically linked to the visual processing of several different types of motion stimuli (Born and Bradley 2005; Riečanskỳ 2004; Zeki 2015) and known to lead to deficits in motion discrimination when lesioned (Barton et al. 1996).

It is noteworthy that fMRI results suggest an involvement of the pre-frontal cortex when participants view an implied motion sequence (Rao et al. 2004), a result taken to support the view that RM reflects high-level cognitive representations of dynamic events (Hubbard 2005). In a similar vein, Amorim et al. (2000), using magnetoencephalography, identified the involvement of a fronto-parietal cortical network in a motion extrapolation task, with trials compatible with a RM effect contingent on an activation of centro-parietal regions of the right hemisphere.

As stated above, given the complex relationship between RM and variations of the inducing stimuli, the task employed to measure it and the variables that modulate its magnitude, it might not be warranted to collapse the available neurophysiological evidence into a single picture. This is particularly true when RM is measured for targets undergoing continuous smooth motion, as is the case in the experiment to be presently discussed, for not only is there scarce available evidence concerning which cortical areas are involved, but the phenomenon is known to be sensitive to extraneous variables, such as the presence of smooth pursuit eye movements (De Sá Teixeira 2016) and the nature of the spatial localization task (De Sá Teixeira et al. 2017).

In what refers specifically to RG, no study to date attempted to identify its neural correlates. In part, this is because RG has been far less studied than RM. Also, and until recently, empirically disentangling both phenomena was not always straightforward, for they jointly determine the measured spatial displacement. Nevertheless, parallel research lines, the bulk of which has focused on human abilities to either intercept a falling object (Bosco et al. 2012; La Scaleia et al. 2014, 2015; Lacquaniti and Maioli 1987, 1989; McIntyre et al. 2001) to estimate time-to-contact or to intercept a virtual target subjected to gravity-congruent dynamics (Delle Monache et al. 2014; Moscatelli and Lacquaniti 2011; Zago and Lacquaniti 2005) have amassed considerable evidence favouring the hypothesis that the brain implements an internal model of gravity, which outputs predictions for the effects of Earth gravity (Bosco et al. 2015; Lacquaniti et al. 2013, 2014, 2015; Zago and Lacquaniti 2005). What is more, a network of brain regions, within and in close vicinity to the Temporo-Parietal Junction (TPJ), has been identified and linked to the functioning of an internal model of gravity, both with the aid of fMRI (Indovina et al. 2013; Indovina et al. 2005; Maffei et al. 2010), TMS (Bosco et al. 2008; Delle Monache et al. 2017), studies of patients with cortical damage (Maffei et al. 2016), and vestibular stimulation (Indovina et al. 2005, 2015; for a meta-analysis see Lopez et al. 2012). As such, this region has been taken as a critical site of the vestibular cortex specifically devoted to the multisensory integration of gravitational cues, and involved in the visual anticipation of gravity effects (Bosco et al. 2015; Lacquaniti et al. 2013, 2014). To the degree that RG likewise reflects the functioning of an internal model of gravity (De Sá Teixeira et al. 2013), it is plausible to hypothesize that it may be modulated by similar neural substrates.

The present study

Our main aim was to ascertain the role played by hMT/V5+ and TPJ cortical areas in modulating the magnitudes of RG and RM. Although the review above does not afford any strong predictions, available evidence does hint that disrupting cortical activity in hMT/V5+ might likely result in a decreased RM. Likewise, it is plausible to hypothesize for RG to be lessened when cortical activity in TPJ is disrupted. To test these hypotheses, a TMS study, employing an offline (that is, not contingent on the execution of the task) continuous Theta-Burst Stimulation (cTBS; Fiori et al. 2015; Huang et al. 2005; Ridding and Ziemann 2010; Sacheli et al. 2015) protocol, was designed in which the target cortical areas of the right hemisphere were selectively disrupted while observers performed a standard spatial localization task. Blocks of trials performed during the lasting cTBS effects were interspersed with no-stimulation blocks, conforming to two partially superimposed Baseline-cTBS–Recovery designs, one for each target cortical area. The logic underlying the adoption of this design was to allow identification of the effects of disrupting cortical activity of each area while still being able to discard non-specific sources of variation related to the stimulation itself. For measurement of RM and RG, we adopted a behavioural spatial localization task, where participants had to indicate the perceived vanishing location of the target. The reason for this choice was twofold: (i) despite its generalized use (Hubbard 2005, 2010, 2014, 2015), it is still to be determined what role, if any, do hMT/V5+ and TPJ play in this task; (ii) with an appropriate design (De Sá Teixeira 2016), this task allows one to obtain specific and independent estimates of RM, linked to the perceived target motion axis, and RG, rooted on an internal reference system independent of motion trajectory and the actual direction of gravity, for any conceivable target trajectory. Finally, and besides measuring spatial localization errors, eye movements were tracked and relevant oculomotor features (pursuit gain and oculomotor overshoot) subjected to a similar analysis.

Method

Participants

22 volunteers (12 males), with ages between 22 and 52 ($M = 27.9$; SD = 6.7), were paid €40 to take part in the experiment. All of them had normal or corrected to normal vision, were right-handed, had no known neurological deficits and fulfilled the safety criteria for enrolment in a TMS study (Rossini et al. 2015; Wasserman 1998). Sample size was estimated based upon previous related studies (Delle Monache et al. 2017; De Sá Teixeira 2016).

Stimuli

A simple animation involving a black circle (target) with a diameter of 30 pixels (0.78°), moving linearly at a constant speed of 600 pixels per second (px/s; 15.59°/s) on an otherwise white background, was used as stimulus. On each trial, the orientation of the target trajectory could vary between 0° (rightward), 22.5°, 45°, 67.5°, 90° (upward), 112.5°, 135°, 157.5°, 180° (leftward), 202.5°, 225°, 247.5°, 270° (downward), 292.5°, 315° or 337.5°. The trajectory length was 600 pixels (15.59°), but randomly positioned on the screen such that the target vanished inside an area of 50 (1.31°) squared pixels at about 90 pixels (2.35°) beyond the centre of the screen. A cross-shaped cursor, the position of which could be adjusted with a mouse, appeared on the centre of the screen immediately after target offset.

Apparatus and equipment

Stimuli were presented on a 22″ LCD screen (Viewsonic VX2268WM, 16:9) with a resolution of 1680 × 1050 px (46 × 26 cm) and a refresh rate of 100 Hz. A black cardboard mask obstructed the view of the screen except for a circular area with a diameter of 26 cm (24.45º). Participant's head movements were restrained with a chin rest and forehead support at 60 cm from the screen, with the direction of their cyclopean eye aligned with its centre. Programming of the experiment, stimuli presentation, trial randomization and collection of localization responses was done with Presentation (v. 14.9, Neurobehavioral Systems, USA). Localization responses were performed with a modified gaming mouse (Razer Copperhead, Razer USA), allowing a 1 ms temporal resolution for button presses (via a data acquisition interface; CED Power 1401), with position of the cursor sampled at 200 Hz through the USB port. During each block, participants were acoustically isolated with white noise continuously delivered through in-ear earphones (Bose, USA; loudness was adjusted on an individual basis to mask any surrounding noises without being disruptive to the participant) and the laboratory room kept in darkness. Eye movements were binocularly recorded with a remote EyeLink 1000 tracker (SR research, CA) at a sampling frequency of 500 Hz. Transcranial magnetic stimulation was delivered through a figure-of-eight coil (Double 70 mm coil; mounted on a multiple degrees of freedom mechanical arm; Magic Arm, Manfrotto Italy) attached to a SuperRapid^2 stimulation unit (Magstim, Whitland, Wales, UK) and positioned on the participant's scalp aimed at the target sites with the aid of Brainsight neuronavigation system (Rogue Research, CA).

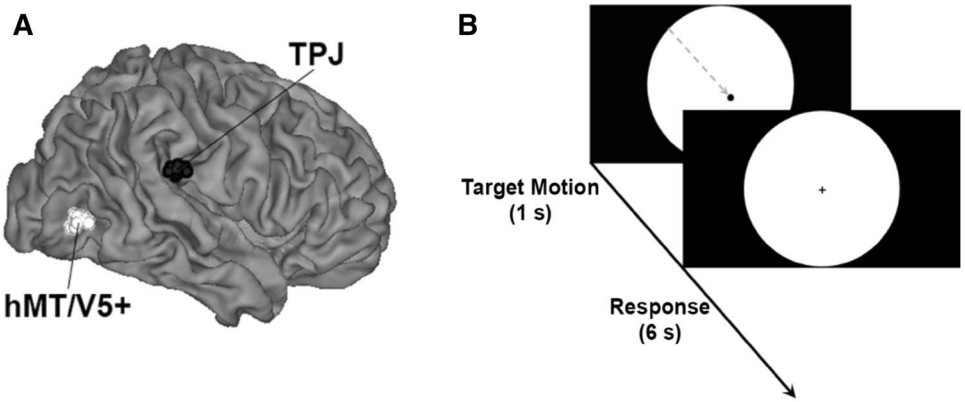

Fig. 1 **a** Individual target cortical sites represented over CARET's 3D fiducial rendering of the MNI brain template (Van Essen et al. 2001); **b** schematic depiction of one spatial localization trial

Procedure and design

Each cortical area of interest (hMT/V5+ and TPJ) was identified a priori on the right hemisphere in a normalized stereotactic space based upon individual MRI anatomical brain images acquired on a Siemens Magnetom Allegra 3 Tesla head-only scanning system (Siemens Medical Systems, Erlangen, Germany). For stimulation of TPJ, MNI coordinates $X=67$, $Y=-26$ and $Z=23$ were targeted (see Fig. 1a, black dots; cf. Bosco et al. 2008; Delle Monache et al. 2017). As for hMT/V5+, the TMS coil was positioned at MNI coordinates $X=52$, $Y=-71$ and $Z=0$ (see Fig. 1a, white dots; Bosco et al. 2008; Orban et al. 2003). Upon arrival at the laboratory, participants were briefed about the experimental procedure, screened for the TMS safety criteria (see Rossini et al. 2015; Wasserman 1998) and asked to sign an informed written consent form. All procedures were approved by the local ethics committee (protocol 169/16). A licensed medical doctor was present in the laboratory during all TMS procedures. No participant experienced any adverse effect when subjected to the stimulation protocol. In each trial (see Fig. 1b), participants were instructed to pay attention to the target and, upon its offset, to locate with the mouse its vanishing position on the screen (confirmed with the left button), as precisely as possible. The next trial started 6 s after the vanishing of the target, thus ensuring both time for each localization response as well as a duration of no more than 20 min for an entire block, comprised of 160 trials (16 target motion trajectories × 10 repetitions). Eye tracking calibration was performed at the start of each block and after the completion of 80 trials, while drift corrections were made every 20 trials. No instructions concerning gaze behaviour were provided. Each participant performed two experimental blocks, one for each target cortical area of interest (hMT/V5+ and TPJ), following a cTBS protocol consisting of a train of triplets of pulses at 50 Hz every 200 ms for 20 s at 50% of the maximum stimulator output. This protocol was estimated to disrupt cortical activity for about 20 min (lasting for a maximum for 30 min; cf. Fiori et al. 2015; Huang et al. 2005; Sacheli et al. 2015; for a review, see Wischnewski and Schutter 2015). The mean error in coil positioning across all participants was 0.488 mm (SD = 0.144; Maximum = 0.764) and 0.683 mm (SD = 0.298; Maximum = 1.197) when targeting TPJ and hMT/V5+, respectively.

To assess the effects of cortical activity disruption, each cTBS block was performed after and before blocks with no cortical stimulation, to establish, respectively, a baseline and recovery performance. Overall, each participant was thus subjected to two concatenated repeated-measures baseline-cTBS-recovery designs, one for each target cortical area (hMT/V5+ and TPJ) and with order of stimulated area counterbalanced between participants. Aiming to maintain the duration of the experimental session within reasonable limits and so as to not unnecessarily tire participants with the successive repetition of the same task, the two baseline-cTBS-recovery blocks were partially superimposed such that the recovery block for the first cortical area and the baseline block for the second cortical area were collapsed into one single experimental block. Therefore, and in total, each participant performed 5 experimental blocks. The first block was performed without transcranial magnetic stimulation to establish a baseline performance for the first cortical area to be stimulated. Prior to the start of the second block (but after the eye tracking calibration), a cTBS protocol (see above) was employed, targeting the first cortical area of interest (hMT/V5+ for half the participants, TPJ for the remaining). 40 min after the end of the cTBS protocol (to allow the return of cortical activity towards normal levels), a third experimental block was administered—this block was taken both as a recovery condition for the first target area and as the baseline for the second cortical target site. The fourth block was again preceded by an offline cTBS protocol applied to the remaining cortical area of interest (TPJ or hMT/V5+). Finally, a fifth block, starting again 40 min after the end of the cTBS protocol, was run and taken as the recovery condition for the second cortical target site. The entire experimental session lasted about 3 h.

Data analysis

Prior to data analysis, outlier localization responses within each individual combination of block and motion direction were discarded, based upon a cut-off value of 2 standard-deviations above or below the mean. This cut-off point was found, in preliminary analysis, to be effective in discarding responses reflecting accidental presses of the mouse button without significantly altering the means of the "true" responses. Less than 2% of the total number of trials were so discarded. For the remaining trials, the arithmetic difference between the horizontal and vertical coordinates of the localization response and the coordinates of the actual vanishing position were calculated. The obtained differences were used to determine the displacement along the motion trajectory, M-displacement, in pixels (1 pixel $\approx 1.56'$), such that positive values corresponded to localizations further beyond the target actual offset. At this point it should be noticed that both RM and RG jointly determine *M*-displacement values, with the relative contribution of the latter varying with target motion direction from a null value, for targets moving orthogonal to the subjective vertical direction, to a maximum, for targets moving along the subjective vertical direction, and to a minimum, for targets moving against the subjective vertical direction. Arguably, for an upright healthy observer, the subjective vertical direction would be roughly aligned with the Earth gravitational pull, although it is important to conceptually distinguish between the two. Theoretically, *M*-displacements would thus be expected to fluctuate sinusoidally, as a function of the target motion directions, reflecting the contribution of RG, and around a positive constant value, corresponding to RM magnitude (for details see, e.g., De Sá Teixeira 2016).[1] By virtue of the Fourier theorem, a set of *M*-displacements, measured for each of *n* possible motion directions, may be expressed as a sum of periodic terms of increasing frequency, as follows:

$$\begin{aligned} M(\theta) = {} & c + b_1 \sin\left(\theta/2\pi\right) + a_1 \cos\left(\theta/2\pi\right) \\ & + b_2 \sin\left(2\theta/2\pi\right) + a_2 \cos\left(2\theta/2\pi\right) + b_3 \sin\left(3\theta/2\pi\right) \\ & + a_3 \cos\left(3\theta/2\pi\right) + \ldots + b_n \sin\left(n\theta/2\pi\right) + a_n \cos\left(n\theta/2\pi\right) \end{aligned} \quad (1)$$

Constant c reflects a constant magnitude common to all motion directions and, thus, indexes RM. Coefficients a_{1-n} and b_{1-n} reflect the magnitude of sine and cosine terms, respectively, of frequencies $n/2\pi$. Setting the rightward, upward, leftward and downward motion directions as 0º, 90º, 180º and 270º, respectively, coefficient a_1 expresses a rightward (0º) increase of *M*-displacements, b_1 an upward increase (90º; relative contributions of a_1 and b_1 index increases of *M*-displacements along any one possible direction), a_2 a horizontal increase of *M*-displacements (both rightward, 0º, and leftward, 180º), b_2 a vertical increase (both upward, 90º, and downward, 270º), b_3 and a_3 increases of *M*-displacement along three main directions, a_4 and b_4 along four main directions, and so forth. Importantly, such a set of direction-dependent *M*-displacements can be subjected to a Fourier decomposition procedure (see Sekuler and Armstrong 1978), with which constant c and harmonic coefficients (a_n and b_n) of Eq. 1 can be independently determined. Within this logic, previous studies (De Sá Teixeira 2016) showed that *M*-displacements can be reasonably described by a positive constant c plus a sin (θ) component modulated by a negative b_1 coefficient and a cos (2θ) function with magnitude a_2:

$$M(\theta) = c - b_1 \sin\left(\theta/2\pi\right) + a_2 \cos\left(2\theta/2\pi\right) \quad (2)$$

Equation 2 states that M-displacement results from the combination of a tendency to locate the offset of a target displaced forward in the direction of motion (c)—RM—, a trend to perceive offset positions displaced downward (b_1)—RG—, and a somewhat increased forward displacement for horizontally moving targets (a_2). The same procedure was employed in the present experiment: for each participant, the set of *M*-displacements were averaged across repetitions and subjected to a discrete Fourier decomposition procedure (Sekuler and Armstrong 1978). All harmonic coefficients up to a frequency of $4/2\pi$ were estimated and percentage of variance explained used to determine which accounted for the main trends in *M*-displacement. The same procedure was also employed for the analysis of individual mean response times.

For eye tracking recordings, data collected during blinks were discarded. Eye position data were filtered by means of a 2nd order Butterworth filter (cut-off frequency of 40 Hz), averaged across the left and right eyes to find the cyclopean eye direction, converted to pixel coordinates in relation to the target offset, and gaze location along the target's motion axis calculated. Trials where participants smoothly tracked the target while it was visible were identified and smooth pursuit gain calculated (a gain of 1 indicates that the eyes speed matched target speed, while lower values indicate that eyes speed was lower than target speed). Percentage of trials where the target was smoothly tracked and smooth pursuit gain were taken as dependent variables and subjected to statistical analysis in all respects similar to the ones employed for *M*-displacement and response times.

[1] The terms "M-displacement" and "forward displacement" will be used, in the present paper, interchangeably and will be reserved for the empirically observed localization errors, with RM and RG referring to theoretical constructs hypothesized to modulated the latter, biasing the perceived offset forward, in the direction of (seen) motion, and downward, in the direction of (perceived) gravity, respectively.

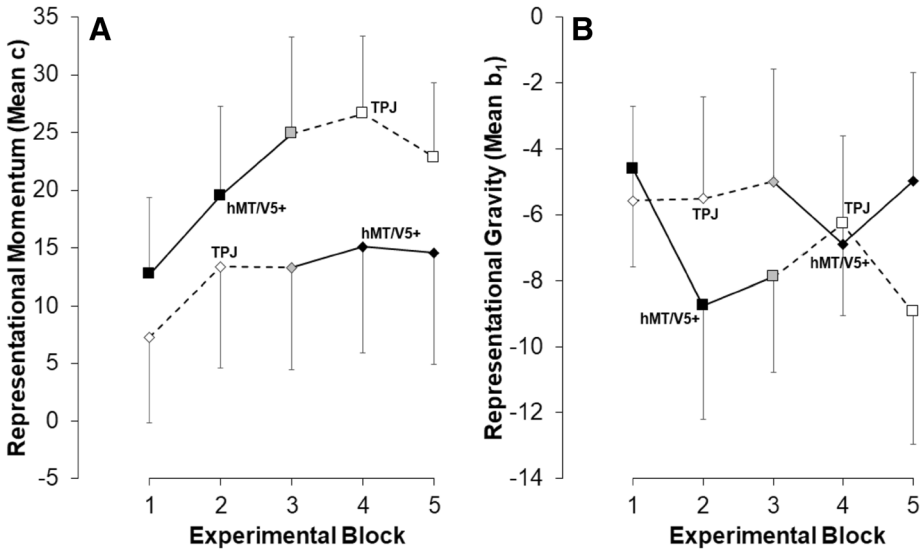

Fig. 2 Mean individual c constants (RM; **a**) and b_1 coefficients (RG; **b**) as a function of experimental block for both order groups (hMT/V5+ first—square markers; TPJ first—diamond markers). Data labels identify, for the cTBS blocks, which cortical area was stimulated. Error bars depict the standard errors of the subgroup means

Preliminary analysis revealed that participants' eyes kept moving for at least 200 ms after the target vanished, in those cases where it was smoothly tracked. In a significant percentage of cases, participants made a saccade to the centre of the screen (where the mouse cursor appeared) roughly 200–300 ms after the target disappeared. Thus, and to explore patterns of ocular overshoot, trials where the target was being smoothly tracked for at least 100 ms before the target disappeared were identified and mean gaze location during slots of 10 ms (the duration of each frame in the presentation screen) was calculated at 0 (when the target vanished), 50, 100, 150 and 200 ms after target offset. Magnitude of ocular overshoot, in pixels, was subjected to the same discrete Fourier decomposition procedure employed for the remaining dependent measures.

For all measures (M-displacement, Response Times and eye tracking recordings) and each cortical area of interest (hMT/V5+ and TPJ), the relevant estimated harmonic parameters were taken as dependent measures and subjected to mixed ANOVAs with condition (baseline-cTBS-recovery) as the repeated-measures factor (for magnitude of ocular overshoot only, time elapsed after target's offset was taken as an additional repeated-measures factor) and order of stimulated cortical areas as the between-subjects factor.

Results

Spatial localizations

In accordance with previous findings (De Sá Teixeira 2014, 2016), M-displacements were well described by a sum of a constant c (indexing RM), a $\sin(\Theta/2\pi)$ function modulated by a negative coefficient b_1 (indexing RG) and a $\cos(2\Theta/2\pi)$ component modulated by a coefficient a_2 (signalling that M-displacements were overall bigger for horizontal than vertical directions; cf. Eq. 2). These harmonic components accounted for more than 97% of the variation in M-displacement as a function of motion direction for all experimental blocks. Preliminary analysis revealed that the coefficient a_2 did not vary significantly across experimental blocks for both cortical areas of interest ($p > 0.1$). Thus, it will not be discussed further.

As for the remaining spatial localization dependent variables, Fig. 2 depicts mean RM (c parameter) and mean RG (b_1 parameter) as a function of experimental block, plotted separately for both order groups. Data labels indicate which cortical area (hMT/V5+ or TPJ) was stimulated prior to the associated block. Visual inspection suggests that, overall, RM tended to increase with each successive block. This trend is clearly seen for the initial experimental blocks, especially for those participants for whom hMT/V5+ was targeted first (see Fig. 2a, black squares). When cTBS was applied to TPJ mean RM seems to be slightly increased, deviating from that linear trend (see Fig. 3a, white markers, inverted V trends). Conversely, disruption of cortical activity in hMT/V5+ seems to lead to an increase in the magnitude of RG (see Fig. 2b, black markers, V trends).

Aiming to isolate possible effects of cTBS from the clear sequential fluctuations along the experimental blocks, mean RM (c parameter) and mean RG (b_1 parameter) were subjected, as dependent variables, to mixed ANOVAs, separately performed for each cortical area of interest (hMT/V5+ and TPJ) with condition (baseline-cTBS-recovery) as the repeated-measures factor and order of stimulation (hMT/V5+ – TPJ or TPJ – hMT/V5+) as the between-subjects factor. Since the levels of the factor condition are taken in a fixed order (baseline – $cTBS$ – recovery), within-subjects contrasts can be used to differentiate between sequential effects, reflecting the mere repetition of the task across

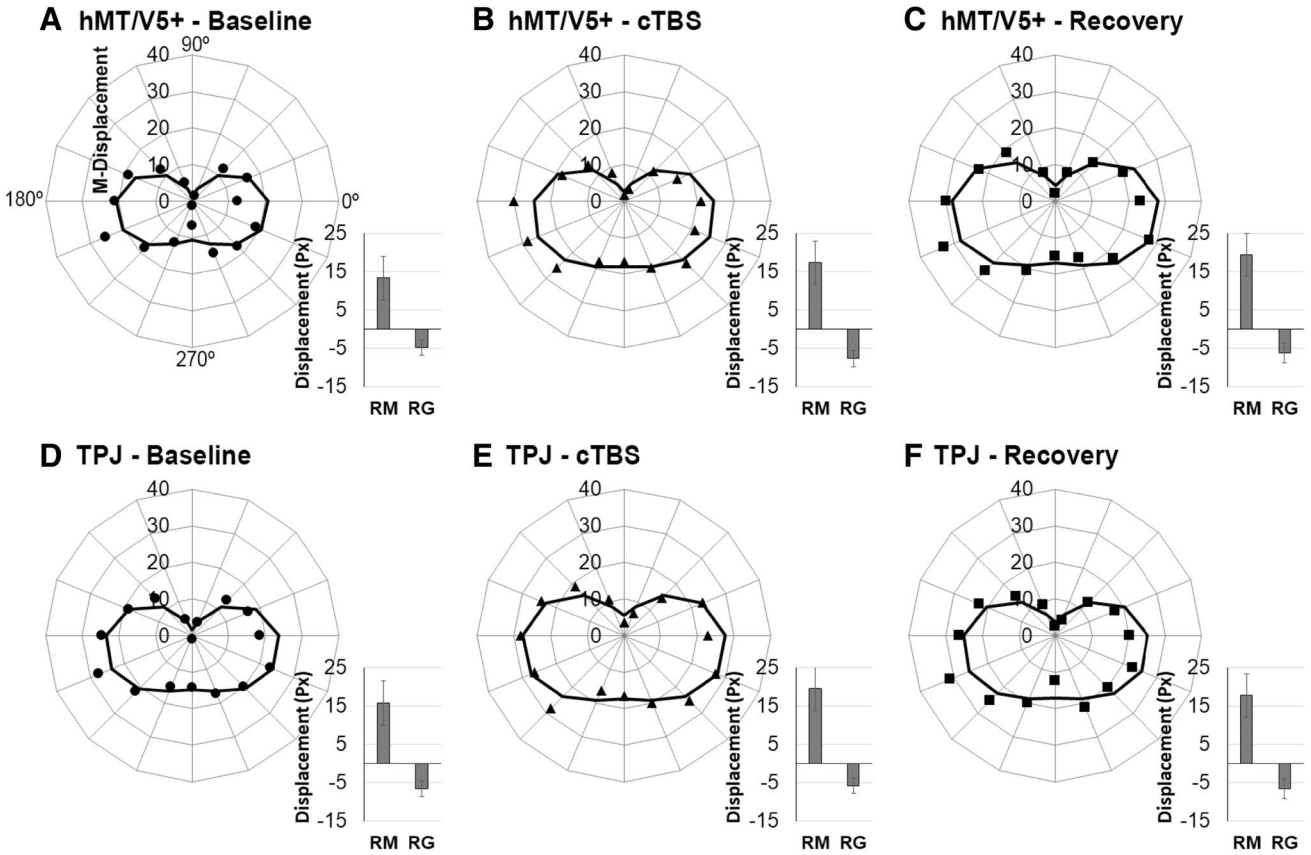

Fig. 3 Mean *M*-displacements as a function of motion direction found for the baseline (left column; circle markers), cTBS (middle column; triangle markers) and recovery (rightward; square markers) blocks for target cortical sites hMT/V5+ (top row) and TPJ (bottom row). The full lines are the best fit Fourier model. Inset plots depict mean RM (c) and RG (b_1) for each condition

blocks, and effects due to the disruption of cortical activity. The former would reflect on a significant linear contrast (continuous increasing or decreasing of the dependent variable as a function of condition) and the latter on a significant quadratic contrast (signalling either an increase or a decrease of the dependent variable in the middle condition, that is, the cTBS block).

Regarding hMT/V5+, RM (c parameter) was found to increase significantly with each successive block (condition), $F(2, 40) = 10.84$, $p < 0.001$, partial $\eta^2 = 0.35$ (linear contrast: $F(1, 20) = 14.04$, $p = 0.001$, partial $\eta^2 = 0.41$; quadratic contrast: $F(1, 20) = 1.09$, $p = 0.309$). This effect was modulated by the order in which cortical areas were stimulated, as revealed by a significant interaction between condition and order of stimulation, $F(2, 40) = 6.94$, $p = 0.003$, partial $\eta^2 = 0.26$, being considerably more pronounced for those participants who performed first the hMT/V5+ sequence of blocks. As for RG (b_1 coefficient), disrupting the activity of area hMT/V5+ was found to significantly increase its mean magnitude, as revealed by a main effect *of condition*, $F(2, 40) = 3.9$, $p = 0.029$, partial $\eta^2 = 0.16$, with a null linear contrast, $F(1, 20) = 1.98$, $p = 0.175$, but a significant quadratic contrast: $F(2, 40) = 6.54$, $p = 0.019$, partial $\eta^2 = 0.25$. The latter effect did not interact with order of stimulation, $F(2, 40) = 1.19$, $p = 0.316$, being found for both subgroups of participants.

As for TPJ, disruption of its cortical activity resulted in an increased RM, as revealed by a significant main effect of condition, $F(2, 40) = 3.28$, $p = 0.048$, partial $\eta^2 = 0.14$, with a null linear contrast, $F(1, 20) = 1.4$, $p = 0.251$, and a significant quadratic contrast: $F(1, 20) = 6.175$, $p = 0.022$, partial $\eta^2 = 0.24$. Moreover, there was also a significant interaction between order of stimulation and condition, $F(2, 40) = 3.54$, $p = 0.038$, partial $\eta^2 = 0.15$, suggesting that RM, besides being increased contingently with the stimulation of TPJ, also increased linearly with each successive block for those participants who were first subjected to cTBS in TPJ area, in contrast with those for whom this area was stimulated last (linear contrast: $F(1, 20) = 5.83$, $p = 0.025$, partial $\eta^2 = 0.23$; quadratic contrast: $F < 1$). No changes in RG (b_1 coefficient) were found linked with stimulation of TPJ, $F < 1$, and no further main effects or interactions reached the significance level. Finally, there

was no evidence that order of stimulated areas had any significant main effect in all conducted analyses.

Figure 3 depicts, in polar plots, the mean *M*-displacements as a function of target motion direction for the baseline (left column, circular markers), *cTBS* (middle column, triangular markers) and recovery (right column, squared markers) conditions for the cortical areas hMT/V5+ (upper row) and TPJ (lower row). The black lines depict the best fit Fourier function. Inset plots depict mean c (RM) and b_1 (RG) parameters for each condition. In accordance with statistical analysis, and besides a visible increase of the magnitude of RM with each successive block, it seems to also increase beyond that linear trend when the activity in TPJ is disrupted (see panel E). As for RG, it seems to be slightly increased for the condition where cortical activity in hMT/V5+ was disrupted (see panel B).

To identify participants responsive to cTBS and who thus contributed more to the found effects, individual c and b_1 parameters were transformed to normalized Z values for the baseline-cTBS-recovery sequences of hMT/V5+ and TPJ. The resulting values were then subjected to a combination of hierarchical cluster analyses (furthest neighbour clustering algorithm based upon a Squared Euclidean Distance metric) and visual inspection of individual patterns. On what refers to hMT/V5+, 14 out of 22 participants showed an increased RG (b_1) following the cTBS protocol. The remaining 8 participants showed either a trend where RG (b_1) decreased in the cTBS block (3 participants), a continuous decrease of RG (b_1) with each successive block (2 participants), or a continuous increase of RG (b_1) with each successive block (3 participants). This pattern of frequencies deviated significantly from chance, $\chi^2(3) = 18$, $p < 0.001$. Similarly, for TPJ, 14 participants displayed increased values of RM (c) during the cTBS block. From the remaining 8 participants, 4 participants showed a decreased RM (c) following the cTBS protocol, 3 participants had measured RM (c) decreasing with each successive block, and for one participant RM (c) increased with each successive block. The frequency of increased RM (c) following disruption of the activity of TPJ significantly deviated from chance, $\chi^2(3) = 18.36$, $p < 0.001$. Overall, 17 participants showed either one of those trends, 11 of whom showed both. Figure 4 depicts the individual Z normalized values of constants c (panels A and B) and coefficients b_1 (panels C and D) as a function of the baseline-cTBS-recovery sequences associated with stimulation of cortical areas hMT/V5+ (panels A and C) and TPJ (panels B and D). Full lines in plots B and C identify those participants who showed, respectively, a tendency for higher RM following TPJ stimulation and higher RG after stimulation of hMT/V5+.

Although statistical analysis supports an effect of disrupting cortical areas hMT/V5+ and TPJ on the magnitudes of RG and RM, respectively and as revealed by significant

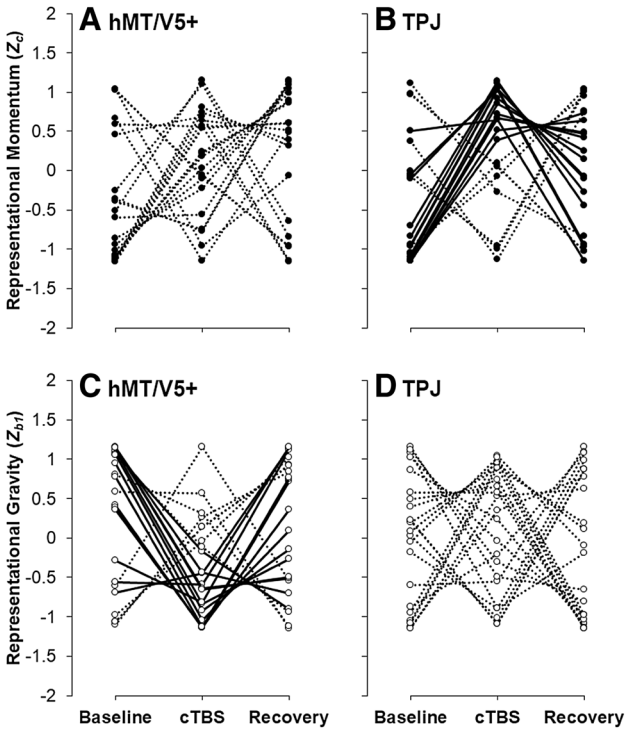

Fig. 4 Individual Z normalized values of RM (constants c; **a**, **b**) and RG (b_1 coefficients; **c**, **d**) as a function of block (baseline, cTBS and recovery) for cortical areas hMT/V5+ (**a**, **c**) and TPJ (**b**, **d**). Full lines in **b** and **c** identify those participants who showed some responsiveness to cTBS in accordance with the main statistical outcomes

quadratic contrasts, it is also the case that the successive repetition of the task leads to lawful variations of the spatial displacement phenomena. The latter is particularly evident for RM in the first performed blocks, which was found to steadily increase in magnitude with each repetition of the task.

Aiming to isolate variations in both phenomena linked specifically to the cTBS procedure, the relative displacement change was computed for each participant as follows: b_1 and c estimates were averaged across the baseline and recovery blocks (thus obtaining the best estimate for each parameter had no stimulation been applied) and the obtained values subtracted from the b_1 and c estimates found in the cTBS blocks. Figure 5 depicts the mean relative displacement change found for the cTBS blocks for RM (c parameter—dark grey bars) and RG (b_1 coefficient—light grey bars). Overall, and in accordance with the previous analyses, RG seems to be increased when activity in hMT/V5+ was disrupted. Conversely, RM, measured during the effects of cTBS applied to TPJ, was found to be increased, albeit only slightly.

The relative changes in pixels for both RM and RG were subjected to a mixed MANOVA with cortical area (hMT/V5+ and TPJ) as a repeated-measures factor and order of

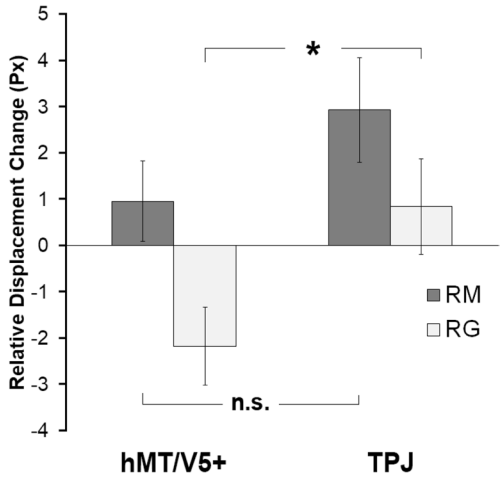

Fig. 5 Relative change in the magnitudes of RM (dark grey bars) and RG (light grey bars) contingent with cTBS, applied either to hMT/V5+ (left bars) or TPJ (right bars), in comparison with the average of the baseline and recovery blocks. Error bars depict the standard errors for the means. Notice that positive and negative values indicate, respectively, an increase in the magnitude of RM and RG contingent with the cTBS block

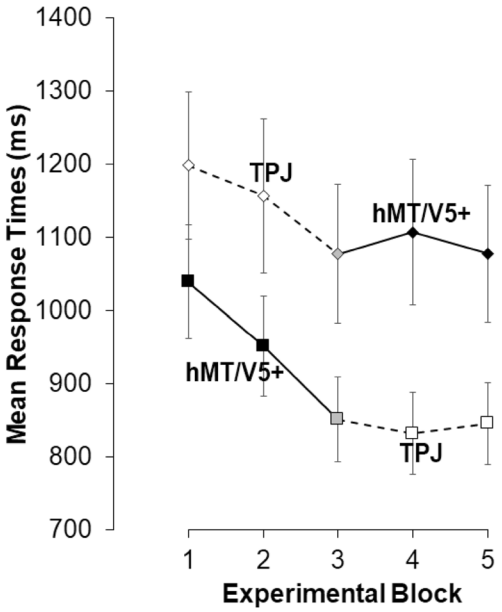

Fig. 6 Mean individual response times as a function of experimental block for both order groups (hMT/V5+ first—square markers; TPJ first—diamond markers). Data labels identify, for the cTBS blocks, which cortical area was stimulated. Error bars depict the standard errors of the subgroup means

cTBS as a between-subjects factor. A multivariate within-subjects effect was found for cortical area, $F(2, 19) = 5.17$, $p = 0.016$, partial $\eta^2 = 0.35$, which did not interact with order of *cTBS*, $F < 1$. Univariate tests revealed that disrupting the cortical activity of hMT/V5+ significantly increased mean relative change in RG in comparison with disruption of activity in TPJ, as revealed with a main effect of cortical area, $F(1, 20) = 6.44$, $p = 0.02$, partial $\eta^2 = 0.24$,. This effect was unchanged as a function of order of *cTBS*, $F(1, 20) = 1.43$, $p = 0.25$. However, mean relative change in RM was not found to be significantly modulated by cortical area, $F(1, 20) = 1.575$, $p = 0.224$, nor by an interaction between cortical area and order of *cTBS*, $F < 1$. No other effects were found to be statistically significant.

Response times

Overall, a single constant in the Fourier series explained above 99% of the variance in response times for all conditions—that is, no evidence was found that response times were modulated by target motion direction and, thus, they were averaged individually across all trials within each block. Figure 6 depicts mean response times for each experimental block. Responses were found to be slower for the very first blocks, decreasing with each iteration of the task. Importantly, there was no evidence that response times deviated from this trend for the cTBS blocks. Two mixed ANOVAs, performed on individual response times separately for each target cortical area (hMT/V5+ and TPJ), with condition (baseline, cTBS and recovery) as the repeated-measures factor and order of stimulated cortical area as the between-subjects factor, corroborated visual inspection. For hMT/V5+, a significant effect of condition was found, $F(2, 40) = 3.725$, $p = 0.033$, partial $\eta^2 = 0.157$ (with a significant linear contrast, $F(1, 20) = 5.16$, $p = 0.034$, partial $\eta^2 = 0.205$) which, moreover, significantly interacted with order of cortical stimulation, $F(2, 40) = 4.4$, $p = 0.019$, partial $\eta^2 = 0.18$. For TPJ, neither condition, $F(2, 40) = 2.57$, $p = 0.089$, nor an interaction between condition and order of stimulation, $F(2, 40) = 2.41$, $p = 0.103$, reached the statistical significance criterion. Taken together, these outcomes reflect a decrease in response times during the first three blocks, being, overall, more pronounced for those participants for whom hMT/V5+ was targeted first.

Eye movements

As expected, and due to the nature of the task, participants routinely engaged smooth pursuit eye movements to track the target throughout its trajectory. In several trials, however, participants either did not track the target at all or tracked it for only short periods (for instance, keeping the gaze at the centre of the screen and tracking the target only once it reached the vicinity, being smoothly tracked afterwards until vanishing). Overall, targets moving horizontally (either leftwards or rightwards), were smoothly tracked while visible and throughout most of its trajectory in about 80% of the trials. In contrast, for targets moving vertically (either

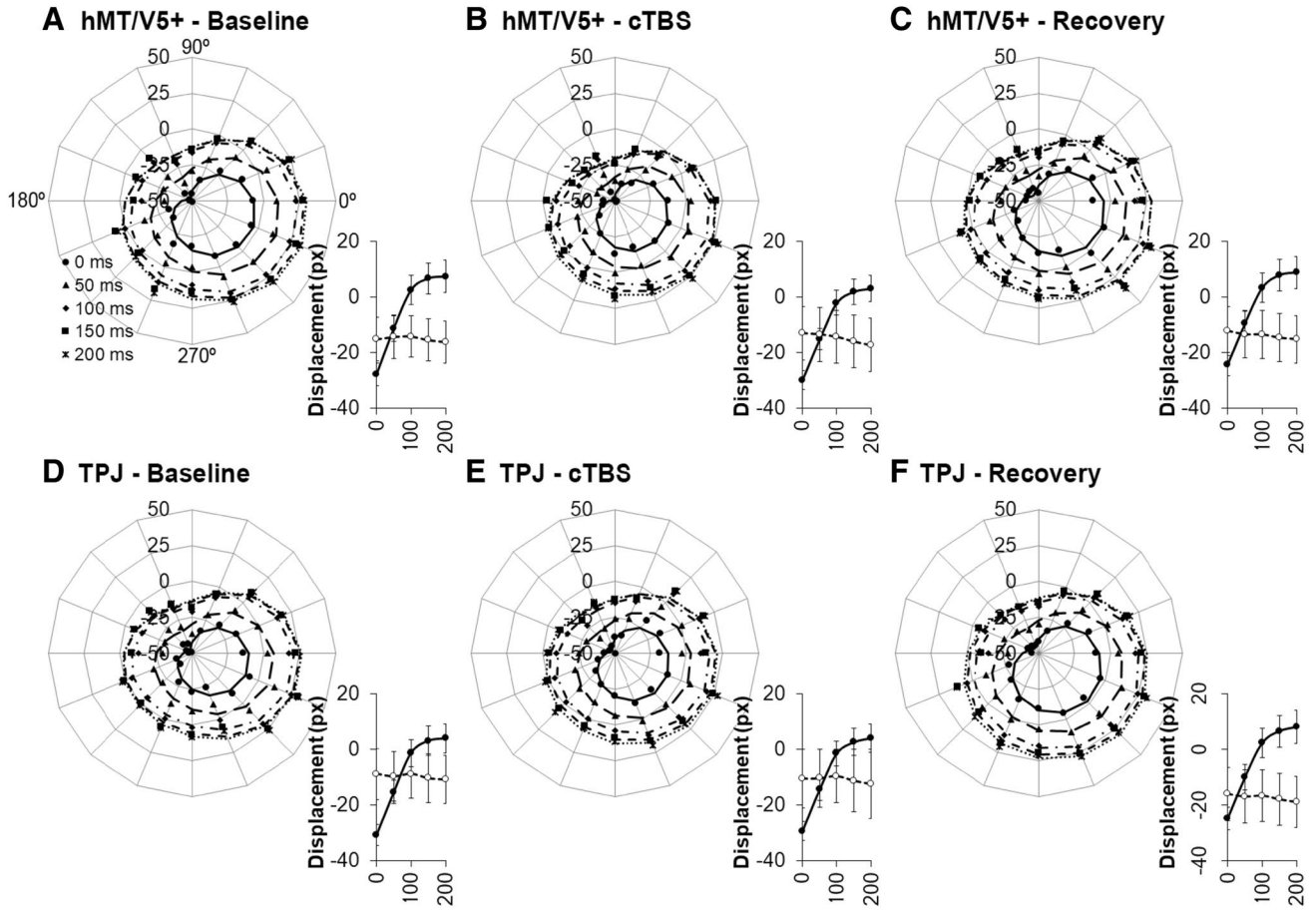

Fig. 7 Mean gaze positions, along the target motion axis and relative to the target actual vanishing location onscreen, as a function of motion direction (radial axes) and time elapsed after target offset (line parameter). The left, middle and right panel columns correspond to the baseline, cTBS and recovery conditions, respectively. Top row panels refer to the hMT/V5+ and the bottom row to the TPJ subdesign. The full lines depict the best fit Fourier models. Lower right insets show, as a function of elapsed time, the mean individual c constants (filled circles and continuous line) and b_1 coefficients (white circles and dashed lines). Error bars represent the standard errors of the means

downwards or upwards), the percentage of smooth pursuit trials decreased to about 60–70% (intermediate percentages applied to targets moving diagonally). Smooth pursuit gain was very close to 1 for horizontally moving targets, but only about 0.6 for vertically moving targets (with intermediate values for targets moving diagonally), in line with previous reports (e.g., Collewijn and Tamminga 1984; Rottach et al. 1996).

Mixed ANOVAs, performed separately for each target cortical site with condition (baseline, cTBS and recovery) as the within-subjects factor and order of stimulated area as the between-subjects factor, revealed that cTBS affected neither the mean percentage of smoothly tracked targets ($F < 1$ when cTBS was applied to hMT/V5+; $F(2, 40) = 1.06$, $p = 0.35$, for cTBS applied to TPJ), nor their mean gains ($F < 1$ for both cortical areas).

In what refers to ocular overshoot, mean gaze position in relation to the actual target offset is plotted in Fig. 7 for each motion direction, time after the target vanished (marker shapes) and condition (Baseline, cTBS and Recovery; panel columns) for each stimulated cortical area (top row: hMT/V5+; bottom row: TPJ). It can be seen that the eyes kept moving forward, in the direction of motion, after the target offset for all motion directions. Moreover, gaze was considerably more displaced in the direction of motion for targets moving rightwards, as compared with leftward directions, and downward, as compared with upward moving targets. All these trends can best be accounted for by a combination of a constant c, harmonic components a_1 and b_1 (lines in polar plots depict the best fit Fourier functions). Together these components accounted for above 90% of the variance in eye position for all blocks. Importantly, stimulation of site hMT/V5+ seems both to decrease the amount by which the eyes overshoot the target offset (see corresponding lower right inset plots, c parameter, filled circles) and to increase the rate at which gaze drift downwards (inset plots,

b_1 parameter, white circles). Conversely, stimulation of TPJ leads to no apparent change in ocular overshoot.

Individual Fourier parameters were analysed through mixed ANOVAs, performed separately for each target cortical site and parameter, with condition (baseline, cTBS and recovery) as the within-subjects factor and order of stimulated area as the between-subjects factor.

When TPJ was stimulated, condition failed to reach the statistical significance level for all dependent variables: constant c, $F(2, 42) = 2.65$, $p = 0.083$; coefficient b_1, $F(2, 42) = 2.08$, $p = 0.14$; coefficient a_1, $F < 1$. For all blocks, and as time after the target offset increased, gaze location was further displaced forward in the direction of motion, $F(4, 84) = 179.4$, $p < 0.001$, partial $\eta^2 = 0.895$, and rightwards, $F(4, 84) = 3.99$, $p = 0.005$, partial $\eta^2 = 0.16$, as revealed by significant main effects of elapsed time after target's offset for the constant c and coefficient a_1, respectively. In contrast, the downward bias of gaze position (as indexed by the coefficient b_1) was found to be relatively stable with time after target offset, $F(4, 84) = 1.86$, $p = 0.124$.

On the other hand, stimulation of site hMT/V5+ significantly reduced mean ocular overshoot—this trend was detected both with a principal effect of condition on mean c, $F(2, 40) = 4.78$, $p = 0.014$, partial $\eta^2 = 0.19$ (with only a significant quadratic contrast, $F(1, 21) = 14.056$, $p = 0.001$, partial $\eta^2 = 0.4$), and with a significant interaction between condition and elapsed time, $F(8, 160) = 2.495$, $p = 0.014$, partial $\eta^2 = 0.11$. Downward gaze displacement (b_1 coefficient) was found to increase with elapsed time, $F(4, 80) = 3.03$, $p = 0.022$, partial $\eta^2 = 0.12$, although mostly due to a significant interaction with *condition*, $F(8, 160) = 3.074$, $p = 0.003$, partial $\eta^2 = 0.13$, in a pattern where stimulation of hMT/V5+ led to a time-dependent downward drift of gaze position. That is, a significant time-dependent downward drift of gaze emerged solely for the cTBS block targeting hMT/V5+. No evidence was found that the rightward gaze displacement (a_1 coefficient) was significantly affected by the cTBS procedure, with condition resulting in a null effect, $F(2, 40) = 1.06$, $p = 0.38$. As was the case for the TPJ conditions, the position of the eyes was found to be further displaced in the direction of motion (c parameter), $F(4, 80) = 160.7$, $p < 0.001$, partial $\eta^2 = 0.889$, and rightwards (a_1 coefficient), $F(4, 80) = 14.18$, $p < 0.001$, partial $\eta^2 = 0.42$, as a function of elapsed time.

Discussion and conclusion

We aimed to explore the role played by areas hMT/V5+ and TPJ on RM and RG. To the degree that hMT/V5+ has been implicated in the processing of motion (Sunaert et al. 1999) and TPJ as a neural substrate for an internal model of gravity for target interception (Bosco et al. 2015; Lacquaniti et al. 2013, 2014), it would be straightforward to expect that disrupting the activity of hMT/V5+ should decrease preferentially RM, whilst disruption of the activity of TPJ should lead to a reduction of the magnitude of RG. Instead, disrupting the activity of hMT/V5+ seems to selectively increase the magnitude of RG, while some evidence was found for a larger RM when disrupting the activity of TPJ. Whereas these outcomes cast doubts on whether hMT/V5+ and TPJ are solely responsible for RM and RG, respectively, and in the sense of its functioning being a sine qua non condition for the emergence of the perceptual displacements, they do provide hints that those neural structures might take part in the modulation of the phenomena.

It should be noticed that cTBS, when targeting hMT/V5+, was also found to reduce the amount by which the observer's eyes overshot the target offset, besides increasing the tendency for gaze to drift downwards after its vanishing. These findings provide evidence that cTBS was effective in disrupting cortical activity. Although not much is known about the neural processes involved in interrupting smooth pursuit eye movements (see Missal and Heinin 2017), both its onset and offset seem to be linked with processes of gain adjustments taking place in the frontal eye fields (FEF; Tanaka and Lisberger 2002a, b). Of relevance, the FEF receives direct inputs from area MT (but not MST, which projects instead to the supplementary eye field area; Missal and Heinin 2017). This could account for our finding that ocular overshoot decreased with stimulation of hMT/V5+, by weakening the processing of retinal motion used in turn for the control of eye movements. Less clear is why hMT/V5+ disruption lead to a downward drift of gaze, although this trend is in line with the found increase in RG, suggesting not only that the two might be linked, but also strengthening the reliability of the latter.

Conversely, we found some evidence that RM increased slightly when the activity of TPJ was disrupted, although this trend was superimposed on a considerable degree of variability. Thus, and on the one hand, statistical analysis revealed that RM increased with each successive repetition of the task, signalled by a significant linear contrast when considering the sequence of baseline-cTBS-recovery blocks. Furthermore, its magnitude was also found to significantly increase, over and beyond that linear trend, when cortical activity in TPJ was disrupted, as evidenced with a significant quadratic contrast. To a great extent, the linear increase in the magnitude of RM can be attributed to training and attentional fluctuations. In fact, it has been reported that RM tends to increase with attentional load (Hayes and Freyd 2002; but see also Kerzel 2004). It is likely that, due to the repetitive design and monotonous nature of the task, participants' attention fluctuated widely during the experimental session, which could, in turn, explain the differences between baseline and recovery blocks. Congruently, mean

response times were also found to steadily decrease during the succession of experimental blocks, reflecting that the spatial localization tasks were performed increasingly more swiftly as the session progressed. However, when attempting to isolate possible RM effects due to cTBS applied to TPJ, by comparing its magnitude in the corresponding block with its mean in the baseline and recovery blocks, a null effect was found. While this latter outcome prevents us from unambiguously stating that the magnitude of RM is significantly modulated by cortical activity in TPJ, it might also be the case that an actual contribution of this cortical area to spatial localization (hinted at by the previous analysis) is being masked by extraneous attentional factors. Without eschewing these considerations and underscoring that a putative link between RM and cortical activity in TPJ is only partially hinted at by the statistical evidence, in the remainder of the discussion we offer a tentative account for the found patterns, taken at their face value.

Overall, a spatial localization can be thought of as reflecting an internal balance between expected kinematics (given the target's motion) and world-based knowledge of dynamic variables (by internally generating an anticipation of gravitational effects). The net effect of disrupting a cortical area involved in the processing of seen kinematics, as can be assumed to be the case of hMT/V5+, could be to compel a heavier reliance upon anticipated dynamics, such as gravity, leading to an increased RG. Conversely, disruption of the functioning of the neural substrates for an internal model of gravity, as could be argued to be the case of TPJ, could lead to a stronger weighting of observed kinematics in fine-tuning the spatial localization, resulting in an enlarged RM. Stated differently, the found results are compatible with a reciprocal functioning between perceived kinematics, involving hMT/V5+ and expected dynamics, with a putative enrolment of TPJ. Disrupting the functioning of one contributing cortical area tips the balance within an extended network, prompting the localization response to rely more heavily on unaffected neural structures.

This sort of reciprocal relationship could, in principle, be functionally modelled as a Bayesian framework (see, e.g., Jörges and López-Moliner 2017) or, neurophysiologically, as an antagonistic mechanism implementing a push–pull dynamic, analogous to some recent proposals. For example, Sestieri et al. (2010, 2017) put forth a similar hypothesis to account for the somewhat paradoxical observation that the posterior parietal cortex, traditionally associated with visuospatial and sensorimotor processes, is also involved in memory retrieval functions, as evidenced with behavioural and neuroimaging studies, even though lesions to this site fail to result in observable amnesic symptomatology (Schoo et al. 2011). As the parietal regions related to perceptual and mnesic functions are anatomically segregated and seem to enter into a dynamic competition (Sestieri et al. 2010), it has been suggested that they show a push–pull relationship, modulated by two possible, and not mutually exclusive, mechanisms: mutual direct suppression or top-down influences from prefrontal regions (Sestieri et al. 2017). Similar competitive neural dynamics have been proposed at a more widespread scale, modulating the interaction between segregated dorsal networks, dedicated to goal-driven attentional processes and including area hMT/V5+, and ventral networks, responsible for stimulus-driven attention and encompassing TPJ (Corbetta and Shulman 2002; Corbetta et al. 2008). Without overemphasizing possible overlaps between anatomical structures and information processing, the reciprocal relation found in the present study, with RM increasing with disruption of TPJ and RG with disruption of hMT/V5+, is compatible with an analogous competitive neural dynamic model.

If one favours this latter account, there are at least two interrelated points of interest. On the one hand, since both RM and RG are simultaneously observed in any single spatial localization response, these phenomena can be instrumental in revealing the degree to which the push–pull mechanisms are due to mutual suppression processes between dorsal and ventral networks or if a top-down modulation is the case. At least in principle, this could be tested by employing an online TMS protocol, targeting either hMT/V5+ or TPJ, with or without previous offline stimulation of pre-frontal areas, previously argued to be enrolled in RM-like tasks (Amorim et al. 2000; Rao et al. 2004). Hypothetically, and to the degree that relevant pre-frontal areas can be pinpointed beyond the currently available evidence, if top-down processes do play a major role in the modulation of a putative push–pull mechanism, it would be expected for the pattern of results to significantly change if the functioning of those areas is compromised. On the other hand, and if such a top-down modulation is indeed the case, a long-standing debate on the literature regarding spatial mislocalizations can be satisfactorily settled. There is still disagreement as to whether RM reflects high-level cognitive representations of motion (Hubbard 2005) or it can be mainly accounted for by low-level perceptual and oculomotor processes (Kerzel 2006; for a reply, see Hubbard 2006). Positing that top-down processes are responsible not for the generation of the localization errors per se, but rather for supervising and modulating the balance between perceived kinematics and anticipated dynamics in determining a spatial localization response could potentially account for the diverging interpretation of the available evidence.

At this point, it should be noticed that at the core of this debate is the role played by smooth-pursuit eye movements. While the necessary involvement of smooth pursuit eye movements in the emergence of RM, at least when gauged for continuous motion and with a spatial localization response, is relatively well established (De Sá Teixeira

2016; De Sá Teixeira et al. 2013; Kerzel 2000, 2003a, c; Kerzel et al. 2001; Müsseler et al. 2002) the debate concerns to what extent oculomotor features are sufficient to explain the phenomenon (Hubbard 2005, 2006; Kerzel et al. 2006). In this respect, the present results do not convincingly support the view that RM fully co-varies with eye movements. Although a significant positive correlation was found between ocular overshoot and RM, disrupting hMT/V5+, which reduced the former, failed to impact significantly on the latter. Conversely, disrupting TPJ, which led to an increase of RM, was not found to significantly change oculomotor behaviour. A push–pull mechanism, as discussed above, might also have a bear on the interpretation of these findings, for a modulation of perceived kinematics and expected dynamics in a spatial localization response is not, in principle, incompatible with a primary causal role of oculomotor behaviour in the former.

As a final remark, and irrespective of how our tentative conclusions might fare in future research, our findings add to previous studies which emphasize the functional independence of RM and RG, and highlight how they are differently modulated by perceived kinematics and expected dynamics.

Acknowledgements This work was supported by the Italian Space Agency (grants I/006/06/0 and MARS-PRE) and the Italian University Ministry (PRIN grants 2015HFWRYY_002, 2017KZNZLN_003 and 2017CBF8NJ_005).

References

Amorim MA, Lang W, Lindinger G, Mayer D, Deecke L, Berthoz A (2000) Modulation of spatial orientation by mental imagery: a MEG study of representational momentum. J Cogni Neurosci 12:569–582

Ashida H (2004) Action-specific extrapolation of target motion in human visual system. Neuropsychologia 42:1515–1524

Barton JJ, Sharpe JA, Raymond JE (1996) Directional defects in pursuit and motion perception in humans with unilateral cerebral lesions. Brain 119:1535–1550

Bertamini M (1993) Memory for position and dynamic representations. Mem Cognit 21:449–457

Born RT, Bradley DC (2005) Structure and function of visual area MT. Ann Rev Neurosci 28:157–189

Bosco G, Carrozzo M, Lacquaniti F (2008) Contributions of the human temporo-parietal junction and MT/V5 + to the timing of interception revealed by TMS. J Neurosci 28:12071–12084

Bosco G, Delle Monache S, Lacquaniti F (2012) Catching what we cannot see: manual interception of occluded fly-ball trajectories. PLoS One 7:e49381

Bosco G, Delle Monache S, Gravano S, Indovina I, La Scaleia B, Maffei V, Zago M, Lacquaniti F (2015) Filling gaps om visual motion for target capture. Front Integr Neurosci 23:9–13

Collewijn H, Tamminga EP (1984) Human smooth pursuit and saccadic eye movements during voluntary pursuit of different motions on different backgrounds. J Physiol (London) 351:217–250

Corbetta N, Shulman G (2002) Control of goal-directed and stimulus-driven attention in the brain. Nat Rev Neurosci 3(3):201–215

Corbetta M, Patel G, Shulman G (2008) The reorienting system of the human brain: from environment to theory of mind. Neuron 58:306–354

De Sá Teixeira NA (2014) Fourier decomposition of spatial localization errors reveals an idiotropic dominance of an internal model of gravity. Vision Res 105:177–188

De Sá Teixeira NA (2016) The visual representations of motion and of gravity are functionally independent: evidence of a differential effect of smooth pursuit eye movements. Exp Brain Res 234(9):2491–2504

De Sá Teixeira NA, Hecht H (2014) Can representational trajectory reveal the nature of an internal model of gravity? Atten Percept Psychophys 76:1106–1120

De Sá Teixeira NA, Hecht H, Oliveira AM (2013) The representational dynamics of remembered projectile locations. J Exp Psychol Hum Percept Perform 39:1690–1699

De Sá Teixeira NA, Kerzel D, Hecht H, Lacquaniti F (2017) A novel dissociation between representational momentum and representational gravity through response modality. Psychol Res 83:1223–1236 **(Epub ahead of print)**

Delle Monache S, Lacquaniti F, Bosco G (2014) Eye movements and manual interception of ballistic trajectories: effects of law of motion perturbations and occlusions. Exp Brain Res 233(2):359–374

Delle Monache S, Lacquaniti F, Bosco G (2017) Differential contributions to the interception of occluded ballistic trajectories by the temporoparietal junction, area hMT/V5+ and the intraparietal cortex. J Neurophysiol 118(3):1809–1823

Fiori F, Candidi M, Acciarino A, David N, Aglioti SM (2015) The right temporoparietal junction plays a causal role in maintaining the internal representation of verticality. J Neurophysiol 114:2983–2990

Freyd JJ (1983) The mental representation of movement when static stimuli are viewed. Percept Psychophys 33:575–581

Freyd JJ, Finke RA (1984) Representational momentum. J Exp Psychol Learn Mem Cogn 10:126–132

Freyd JJ, Finke RA (1985) A velocity effect for representational momentum. Bull Psychono Soc 23:443–446

Freyd JJ, Johnson JQ (1987) Probing the time course of representational momentum. J Exp Psychol Learn Mem Cogn 13:259–269

Freyd JJ, Miller GF (1992) Creature motion. Bull Psychon Soc 30(6):470

Freyd JJ, Pantzer TM (1995) Static patterns moving in the mind. In: Smith SM, Ward TB, Finke RA (eds) The creative cognition approach. MIT Press, Cambridge, pp 181–204

Freyd JJ, Pantzer TM, Cheng JL (1988) Representing statics as forces in equilibrium. J Exp Psychol Gen 117:395–407

Freyd JJ, Kelly MH, DeKay ML (1990) Representational momentum in memory for pitch. J Exp Psychol Learn Mem Cogn 16:1107–1117

Getzmann S, Lewald J, Guski R (2004) Representational momentum in spatial hearing. Perception 33:591–599

Hayes AE, Freyd JJ (2002) Representational momentum when attention is divided. Vis Cognit 9:8–27

Huang ZY, Edwards MJ, Rounis E, Bhatia KP, Rothwell JC (2005) Theta burst stimulation of the human motor cortex. Neuron 45(2):201–206

Hubbard TL (1990) Cognitive representation of linear motion: possible direction and gravity effects in judged displacement. Mem Cognit 18:299–309

Hubbard TL (2005) Representational momentum and related displacements in spatial memory: a review of the findings. Psychon Bull Rev 12:822–851

Hubbard TL (2006) Computational theory and cognition in representational momentum and related types of displacement: a reply to Kerzel. Psychon Bull Rev 13:174–177

Hubbard TL (2010) Approaches to representational momentum: theories and models. In: Nijhawan R, Khurana B (eds) Space and time in perception and action. Cambridge University Press, Cambridge, pp 338–365
Hubbard TL (2014) Forms of momentum across space: representational, operational, and attentional. Psychon Bull Rev 21:1371–1403
Hubbard TL (2015) Forms of momentum across time: behavioral and psychological. J Mind Behav 36:47–82
Hubbard TL, Bharucha JJ (1988) Judged displacement in apparent vertical and horizontal motion. Percept Psychophys 44:211–221
Hubbard TL, Ruppel SE (2002) A possible role of naïve impetus in Michotte's "launching effect": evidence from representational momentum. Vis Cognit 9:153–176
Indovina I, Maffei V, Bosco G, Zago M, Macaluso E, Lacquaniti F (2005) Representation of visual gravitational motion in the human vestibular cortex. Science 308:416–419
Indovina I, Maffei V, Pauwels K, Macaluso E, Orban GA, Lacquaniti F (2013) Simulated self-motion in a visual gravity field: sensitivity to vertical and horizontal heading in the human brain. Neuroimage 71:114–124
Indovina I, Mazzarella E, Maffei V, Cesqui B, Passamonti L, Lacquaniti F (2015) Sound-evoked vestibular stimulation affects the anticipation of gravity effects during visual self-motion. Exp Brain Res 233(8):2365–2371
Jörges B, López-Moliner J (2017) Gravity as a strong prior: implications for perception and action. Front Hum Neurosci 11:203
Kelly MH, Freyd JJ (1987) Explorations of representational momentum. Cognit Psychol 19:369–401
Kerzel D (2000) Eye movements and visible persistence explain the mislocalization of the final position of a moving target. Vis Res 40:3703–3715
Kerzel D (2002) The locus of "memory displacement" is at least partially perceptual: effects of velocity, expectation, friction, memory averaging, and weight. Percept Psychophys 64:680–692
Kerzel D (2003a) Mental extrapolation of target position is strongest with weak motion signals and motor responses. Vis Res 43:2623–2635
Kerzel D (2003b) Attention maintains mental extrapolation of target position: irrelevant distractors eliminate forward displacement after implied motion. Cognition 88:109–131
Kerzel D (2003c) Centripetal force draws the eyes, not memory of the target, toward the center. J Exp Psychol Learn Mem Cogn 29:458–466
Kerzel D (2004) Attentional load modulates mislocalization of moving stimuli, but does not eliminate the error. Psychon Bull Rev 11(5):848–853
Kerzel D (2006) Why eye movements and perceptual factors have to be controlled in studies on "Representational Momentum". Psychol Bull Rev 13:166–173
Kerzel D, Gegenfurtner KR (2003) Neuronal processing delays are compensated in the sensorimotor branch of the visual system. Curr Biol 13:1975–1978
Kerzel D, Jordan JS, Müsseler J (2001) The role of perception in the mislocalization of the final position of a moving target. J Exp Psychol Hum Percept Perform 27:829–840
Kourtzi Z, Kanwisher N (2000) Activation in human MT/MST for static images with implied motion. J Cognit Neurosci 12:48–55
La Scaleia B, Lacquaniti F, Zago M (2014) Neural extrapolation of motion for a ball rolling down an inclined plane. PLoS One 9:e99837
La Scaleia B, Zago M, Lacquaniti F (2015) Hand interception of occluded motion in humans: a test of model-based vs. on-line control. J Neurophysiol 114:1577–1592
Lacquaniti F, Maioli C (1987) Anticipatory and reflex coactivation of antagonistic muscles in catching. Brain Res 406(1–2):373–378
Lacquaniti F, Maioli C (1989) The role of preparation in tuning anticipatory and reflex responses during catching. J Neurosci 9(1):134–148
Lacquaniti F, Bosco G, Indovina I, La Scaleia B, Maffei V, Moscatelli A, Zago M (2013) Visual gravitational motion and the vestibular system in humans. Front Integ Neurosci 7:101
Lacquaniti F, Bosco G, Gravano S, Indovina I, La Scaleia B, Maffei V, Zago M (2014) Multisensory integration and internal models for sensing gravity effects in primates. BioMed Res Int. https://doi.org/10.1155/2014/615854
Lacquaniti F, Bosco G, Gravano S, Indovina I, La Scaleia B, Maffei V, Zago M (2015) Gravity in the brain as a reference for space and time perception. Multisens Res 28:397–426
Lopez C, Blanke O, Mast FW (2012) The human vestibular cortex revealed by coordinate-based activation likelihood estimation meta-analysis. Neuroscience 212:159–179
Luebke AE, Robinson DA (1988) Transition dynamics between pursuit and fixation suggest different systems. Vision Res 28:941–946
Maffei V, Macaluso E, Orban GA, Lacquaniti F (2010) The internal model of visual gravity contributes to interception of real and apparent motion as revealed by fMRI. J Vis 8(6):127
Maffei V, Mazzarella E, Piras F, Spalletta G, Caltagirone C, Lacquaniti F, Daprati E (2016) Processing of visual gravitational motion in the peri-sylvian cortex: evidence from brain-damage patients. Cortex 78:55–69
McGeorge P, Beschin N, Della Sala S (2006) Representing target motion: the role of the right hemispehre in the forward displacement bias. Neuropsychology 20:708–715
McIntyre J, Zago M, Berthoz A, Lacquaniti F (2001) Does the brain model Newton's laws? Nat Neurosci 4:693–694
Missal M, Heinin SJ (2017) Stopping smooth pursuit. Philos Trans R Soc B 372:20160200
Mitrani L, Dimitrov G (1978) Pursuit eye movements of a disappearing moving target. Vision Res 18:537–539
Moscatelli A, Lacquaniti F (2011) The weight of time: gravitational force enhances discrimination of visual motion duration. J Vis 11(4):1–17
Motes M, Hubbard TL, Courtney JR, Rypma B (2008) A principal components analysis of dynamic spatial memory biases. J Exp Psychol Learn Mem Cogn 34(5):1076–1083
Müsseler J, Stork S, Kerzel D (2002) Comparing mislocalizations with moving stimuli: the Fröhlich effect, the flash-lag, and representational momentum. Vis Cognit 9:120–138
Nagai M, Kazai K, Yagi A (2002) Larger forward memory displacement in the direction of gravity. Vis Cognit 9:28–40
Orban GA, Fize D, Peuskens H, Denys K, Nelissen K, Sunaert S, Todd J, Vanduffel W (2003) Similarities and differences in motion processing between the human and macaque brain: evidence from fMRI. Neuropsychologia 41:1757–1768
Pola J, Wyatt HJ (1997) Offset dynamics of human smooth pursuit eye movements: effects of target presence and subject attention. Vis Res 37(18):2579–2595
Rao H, Han S, Jiang Y, Xue Y, Gu H, Cui Y, Gao D (2004) Engagement of the prefrontal cortex in representational momentum: an fMRI study. Neuroimage 23:98–103
Reed CL, Vinson NG (1996) Conceptual effects on representational momentum. J Exp Psychol Hum Percept Perform 22:839–850
Ridding MC, Ziemann U (2010) Determinants of the induction of cortical plasticity by non-invasive brain stimulation in healthy subjects. J Physiol 588:2291–2304
Riečanskỳ I (2004) Extrastriate area V5 (MT) and its role in the processing of visual motion. Ceskoslovenka Fysiologie 53(1):17–22
Rossini PM, Burke D, Chen R, Cohen LG, Daskalakis Z, Di Iorio R, Di Lazzaro V, Ferreri F, Fitzgerald PB, George MS, Hallett M, Lefaucheur JP, Langguth B, Matsumoto H, Miniussi C, Nitsche MA, Pascual-Leone A, Paulus W, Rossi S, Rothwell JC, Siebner HR,

Ugawa Y, Walsh V, Ziemann U (2015) Non-invasive electrical and magnetic stimulation of the brain, spinal cord, roots and peripheral nerves: Basis principles and procedures fro routine clinial and research application—an updated report from an I.F.C.N. Committee. Clin Neurophysiol 126(6):1071–1107

Rottach KG, Zivotofsky AZ, Das VE, Averbuch-Heller L, Discenna AO, Poonyathalang A, Leigh RJ (1996) Comparison of horizontal, vertical and diagonal smooth pursuit eye movements in normal human subjects. Vis Res 36:2189–2195

Sacheli LM, Candidi M, Era V, Aglioti SM (2015) Causative role of left aIPS in coding shared goals during human–avatar complementary joint actions. Nat Commun 6:7544

Schoo LA, van Zandvoort MT, Biessels GJ, Kappelle LJ, Postma A, de Haan EH (2011) The posterior parietal paradox: why do functional magnetic resonance imaging and lesion studies on episodic memory produce conflicting results? J Neurophysiol 5:15–38

Sekuler R, Armstrong R (1978) Fourier analysis of polar coordinate data in visual physiology and psychophysics. Behav Res Methods Instrum 10:8–14

Senior C, Barnes J, Brammer M, Bullmore E, Giampetro V, Simmons A, David AS (1999) The functional neuroanatomy of implicit motion perception. Neuroimage 9(6):s887

Senior C, Ward J, David AS (2002) Representational momentum and the brain: an investigation into the functional necessity of V5/MT. Vis Cognit 9:81–92

Sestieri C, Shulman GL, Corbetta M (2010) Attention to memory and the environment: functional specialization and dynamic competition in human posterior parietal cortex. J Neurosci 30(25):8445–8456

Sestieri C, Shulman GL, Corbetta M (2017) The contribution of the human posterior parietal cortex to episodic memory. Nat Rev Neurosci 18(3):183–192

Sunaert S, Van Hecke P, Marchal G, Orban GA (1999) Motion-responsive regions of the human brain. Exp Brain Res 127(4):355–370

Tanaka M, Lisberger SG (2002a) Role of arcuate frontal cortex of monkeys in smooth pursuit eye movements II: relation to vector averaging pursuit. J Neurophysiol 87:2700–2714

Tanaka M, Lisberger SG (2002b) Enhancement of multiple components of pursuit eye movement by microstimulation in the arcuate frontal pursuit area in monkeys. J Neurophysiol 87:802–818

Van Essen DC, Drury HA, Dickson J, Harwell J, Hanlon D, Anderson CH (2001) An integrated software suite for surface-based analyses of cerebral cortex. J Am Med Inform Assoc 8(5):443–459

Vinson NG, Reed CL (2002) Sources of object-specific effects in representational momentum. Vis Cognit 9:41–65

Wasserman EM (1998) Risk and safety of repetitive transcranial magnetic stimulation: report and suggested guidelines from the international workshop on the safety of repetitive transcranial magnetic stimulation, June 5-7, 1996. Electroencephalogr Clin Neurophysiol 108(1):1–16

White H, Minor SW, Merrell J, Smith T (1993) Representational-momentum effects in the cerebral hemispheres. Brain Cognit 22:161–170

Wischnewski M, Schutter DJLG (2015) Efficacy and time course of theta burst stimulation in healthy humans. Brain Stimul 8(4):685–692

Zago M, Lacquaniti F (2005) Cognitive, perceptual and action-oriented representations of falling objects. Neuropsychologia 43(2):178–188

Zeki S (2015) Area V5—a microcosm of the visual brain. Front Integ Neurosci 9:21